Electr Eng (2012) 94:155–163
DOI 10.1007/s00202-011-0227-1

ORIGINAL PAPER

Gentle synchronization of two-speed synchronous motor with asynchronous starting

Paweł Zalas · Jan Zawilak

Received: 5 November 2009 / Accepted: 20 November 2011 / Published online: 9 December 2011
© The Author(s) 2011. This article is published with open access at Springerlink.com

Abstract The paper presents the results of synchronization calculations for a selected model of the GAe 1716/20t two-speed synchronous motor with switchable armature and field magnet windings, used for driving the main fans in deep mines. The calculations were performed using a specially developed (and validated by measurements) field-circuit model of the motor. The effect of the initial instant of synchronization on the latter's effectiveness and on dynamic process stabilization time was studied. It is shown that synchronization effectiveness can be increased through proper field current control in the synchronization initiation–synchronous speed interval. It is also shown that synchronization time can be reduced and the dynamic waveforms attenuated after the motor reaches the synchronous speed. The calculation results are presented in the form of diagrams.

Keywords Electrotechnology · Synchronous motors · Synchronization process · FEM modelling

1 Introduction

Electromagnetically excited large-power salient-pole synchronous motors are commonly employed in the drive systems of the main-ventilation fans in deep mines. Considering their number and installed capacity, they make up a group of the largest electric energy consumers in the mine. Big savings can be made and the total mining costs can be reduced through the rational use of the fans' capacity. The biggest savings in electric energy can be achieved by changing the rotational speed of the driving machine [1]. The speed of the synchronous motor can be controlled by changing the amplitude and frequency of the supply voltage. But the application of large-power electronic frequency converters still entails high capital costs. The required fan capacity control can also be obtained through the use of two-speed synchronous motors in which a change of speed is effected by changing the number of motor magnetic field poles. Because of the costs, the existing single-speed motors (their magnetic core and mechanical structure) are upgraded for this purpose. The upgrading consists in using a switchable stator winding and rotor winding switching through an additional pair of slip rings [12]. By changing the direction of currents in appropriate groups of stator windings and the polarity of appropriate field-magnet poles, one can obtain another, larger, number of resultant magnetic-field poles and so another, lower, rotational motor speed.

The upgrading is cheaper than the use of large-power converter systems and the stepwise change of speed ensures sufficient capacity control and results in a significant reduction of the power consumed by the fan. One of the motors upgraded in this way is a two-speed synchronous motor of type GAe 1716/20t. Its main specifications and the specification of the single-speed motor are presented in Table 1. By lowering the rotational speed from 375 to 300 rpm, one can reduce the motor's power by over 50% and so considerably reduce the annual energy consumption [4], which will compensate for the upgrading costs.

Since the motors have a salient-pole rotor, then at the two-speed motor's lower speed the number of mechanical poles is different than the number of magnetic poles (respectively, 16 and 20). Due to the fact that the number of magnetic poles is different from that of mechanical poles, the particular poles

P. Zalas (✉)
Institute of Electrical Machines, Drives and Metrology,
Wroclaw University of Technology, ul. Smoluchowskiego 19,
50-372 Wroclaw, Poland
e-mail: pawel.zalas@pwr.wroc.pl

J. Zawilak
e-mail: jan.zawilak@pwr.wroc.pl

Table 1 The ratings of two-speed synchronous motor GAe 1716/20t and single-speed motor GAe 1716t

Motor type (GAe)	1716t	1716/20t	
Rated power (MW)	3.15	2.6	1.2
Stator voltage (kV)	6	6	6
Stator current (A)	350	292	186
Field voltage (V)	90	100	78
Field current (A)	350	337	260
Rotational speed (rpm)	375	375	300
Power factor	0.9 cap.	0.9 cap.	0.77 ind.
Efficiency (%)	96.5	95.5	81.0

are in different magnetic conditions in a given instant (Fig. 4) [3,11]. As a result, the contributions of the particular poles to the generation of driving torque are not equal [2]. Consequently, the drive system's electromechanical time constant and motor slipping increase during asynchronous running, which has a significant influence on synchronization at the lower rotational speed. To increase the pull-in torque, and thereby the effectiveness of synchronization, field current (often 50% higher than the rated current) forcing is commonly used [7,10]. But sometimes, even when field current forcing is employed, no effective synchronization is achieved [11].

The aim of this study is to show that in the adopted motor load conditions, synchronization effectiveness can be increased and the duration of transients reduced through the proper choice of the instant of starting synchronization and through field current control during this process, without using forcing.

2 Field-circuit model of motor

A specially developed field-circuit model of the two-speed motor and Ansoft's Maxwell software were used to analyze the synchronization of the motor [11]. The transient module was used to calculate dynamic transient states. The module also enables one to take the rotary motion of the rotor into account. Because of the motor's large geometrical dimensions and complex structure and the necessity of using a suitably dense finite element mesh, the calculation model was made in two-dimensional space. The mathematical model of the electric machine contains:

- electromagnetic field equations,
- voltage equations describing a three-phase power supply source,
- current equations and
- a motion equation.

The electromagnetic field with motion is described by the following equation [13]:

$$\nabla \times \upsilon \nabla \times A = -\sigma \left(\nabla V_{\mathrm{e}} + \frac{\partial A}{\partial t} - \nu \times \nabla \times A \right) \tag{1}$$

where A is the magnetic vector potential, V_{e} is an electric potential, υ is the reluctivity, σ is the resistivity and ν is the speed of the moving elements.

For two-dimensional models, vector A and ∇V_{e} have only one component in the axis z direction. In this case, scalar potential V_{e} has a constant value in the direction transverse to the conductor. If electric potential gradient ∇V_{e} is written as a difference in potentials V_b between the conductor's beginning and end, Eq. (1) can be expressed as follows [13]:

$$\nabla \times \upsilon \nabla \times A = \sigma \left(\frac{V_b}{l_j} - \frac{\mathrm{d}A}{\mathrm{d}t} \right) \tag{2}$$

where l_j is the length of the machine.

The magnetic field equations are solved in two systems of coordinates: a movable system connected with the rotor and an immovable system connected with the stator. The rotating elements are related to the coordinate system connected with the rotor, which means that the partial derivative of the vector potential is now an ordinary derivative.

In the current equations, one can distinguish conductors where current displacement can be neglected and conductors (e.g., in induction and synchronous motor cages) where current displacement has a significant effect on field distribution. In the former case, current density in the whole conductor volume is the same. To take changes in field sources into account in the calculations, the circuit equations must be solved simultaneously with the field equations. The circuit equations of the windings without current displacement are written as [13]:

$$\pm \frac{N_{\mathrm{c}} l}{Sa} \int \int \frac{\mathrm{d}A}{\mathrm{d}t} \mathrm{d}\Omega + Ri + L \frac{\mathrm{d}i}{\mathrm{d}t} = u_{\mathrm{s}} \tag{3}$$

where N_{c} is the total number of winding conductors, a is the number of armature winding parallel branches, S is the conductor's surface area, u_{s} is the source voltage and i is the winding current intensity.

The first term in Eq. (3) defines the voltage induced in the winding, the second term expresses the voltage drop at winding resistance R and the third term stands for the voltage at inductance L of the coil outhangs.

The voltage equation of the squirrel cage circuits, considered as a multiphase winding, has this form [13]:

$$r_{pn} i_p + l_{pn} \frac{\mathrm{d}i_p}{\mathrm{d}t} = -\mathrm{S}_k \mathrm{S}_k^{\mathrm{T}} V_b \tag{4}$$

and current density J_b in a squirrel cage bar is defined by the following equation [13]:

$$J_b = \sigma \left(\frac{V_b}{l_j} - \frac{\mathrm{d}A}{\mathrm{d}t} \right) \tag{5}$$

where r_{pn} is the resistance of a ring sector between two cage bars, l_{pn} is the inductance of a ring sector between two cage bars, S_k is the matrix of cage bar connections and i_p is the cage bar current intensity.

The current and field equations are discretized in the time domain, which leads to a large and complex nonlinear system of equations. The final system of equations is obtained by coupling the field equations and the circuit equations. Its unknowns are the vector potential values in the discretization grid nodes, the current in the windings and the electric scalar potential between the bar ends. The field and circuit equations are completed with the following equation of motion [13]:

$$J \frac{\mathrm{d}\omega}{\mathrm{d}t} + f\omega = T_\mathrm{E} + T_\mathrm{L} \tag{6}$$

where J is the moment of inertia, ω is the angular velocity of the moving elements, f is the coefficient of friction, T_L is the load torque and T_E is an electromagnetic torque. The electromagnetic torque is calculated by the virtual work method in each time step.

The motion of the rotor in the calculation model of the investigated synchronous machine is represented by slip surface. This calculation method uses two independent finite element meshes for, respectively, movable and immovable parts. Its advantage is that no FEM mesh needs to be generated again in each computational step, which significantly reduces the computing time.

In the 2D model of the synchronous machine, the following were assumed:

- a sinusoidal waveform of supply voltages V_A, V_B, V_C,
- uniform current density in the cross section of the armature winding,
- the machine effective length equal to the stator length and
- real nonlinear core magnetization characteristics.

The geometry of the GAe 1716t motor's magnetic core, which is the same for the single- (Fig. 4a) and two-speed machine (Fig. 4b), was used in the field part of the model. The finite element method (FEM) was used to solve the field equations. The field part of the model was divided into parts with different finite element mesh density. The highest FEM mesh density was used in zones decisive for magnetic field distribution, i.e., in:

- the air gap,
- the stator teeth and
- the pole shoes.

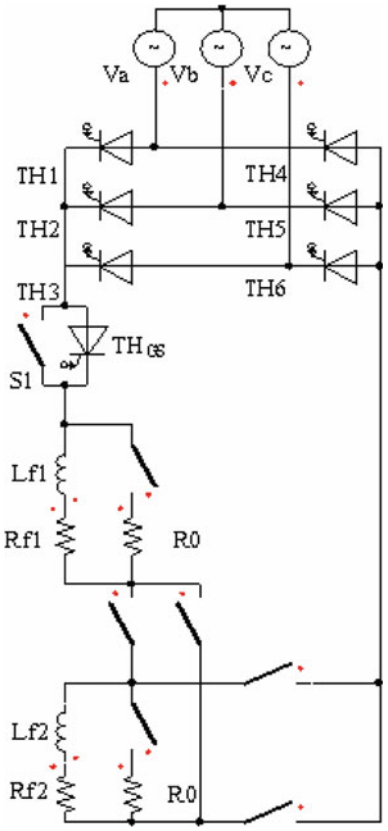

Fig. 1 The circuit part of the model; a diagram of field winding power supply

An analysis of the experimental calculation results showed that the optimal number of finite elements in the 2D model of the investigated synchronous machine was 40,000 knots.

Figure 1 shows the field winding connection diagram of the calculation model circuit part. A starting short-circuiting resistor with a resistance ten times higher than that of the field winding was assumed as R_0. Switches for switching the windings and changing the number of poles and the rotational speed of the motor were incorporated into the circuit model. A static exciter with a controlled six-pulse rectifier was modeled in the field circuit (Fig. 1). Such an exciter is installed in the field circuit of the actual motor [5]. Also, gentle synchronization thyristor $\mathrm{TH_{GS}}$, enabling switching on field voltage in a selected instant, was included (Fig. 1).

To verify the calculation model, measurements on the actual motor installed in a mine fan station and the corresponding calculations [11] were carried out. A comparison of the calculation results with the measurements for:

- the amplitudes and the steady-state phase current harmonic spectrum for two different load torques: $T_\mathrm{L} = 0.4T_\mathrm{N}$ and $T_\mathrm{L} = 0.75T_\mathrm{N}$ at the higher rotational speed and $T_\mathrm{L} = 0.45T_\mathrm{N}$ and $T_\mathrm{L} = 0.8T_\mathrm{N}$ at the lower rotational speed,

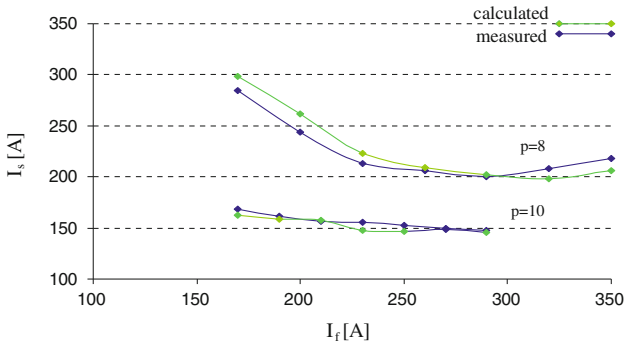

Fig. 2 Calculated and measured curves *V* for the two rotational speeds of the investigated motor

- the shape of the Mordey curves (Fig. 2),
- the active power, the reactive power and the power factor for the different field current values,
- the starting time and the starting current values (Fig. 3),
- the dynamic waveforms of the armature phase currents, the field current, the field-winding-terminal voltage and the rotational speed during synchronization, steady-state work and load torque change,

showed the field-circuit model of the GAe 1716/20t two-speed synchronous motor to be correct and suitable for the further investigation of the phenomena occurring during the operation of motors of this type.

The calculation model was used to determine the motor's electromagnetic field distributions. The calculations were performed for the rotor-relative-to-stator position corresponding to the motor rated load. Figure 4 shows an image of the field generated by the armature winding of, respectively, a single-speed motor (Fig. 4a) and the investigated two-speed motor at the lower rotational speed (Fig. 4b). For this rotational speed of the two-speed motor, the number of mechanical poles is different from the number of magnetic poles (respectively, 16 and 20), which has a significant influence on the synchronization process [11].

3 Synchronization calculations

The two-speed motor runs in the drive of a WPK 5.3 mine fan, whose main specifications are shown in Table 2. Fans of this type, having an outside diameter of about 9 m, are characterized by a high moment of inertia, which is about ten times higher than that of the driving motor's rotor (Table 2). To reduce motor load during synchronization, fan throttling through closing the control unit flaps is used. But in emergency conditions, it is necessary to start the drive unit without air flow throttling. This results in a large load torque, which is the most common cause of difficulties with synchronization at the lower rotational speed of the investigated motor.

The field-circuit model was used to calculate the processes of synchronization up to the two-speed motor's lower synchronization speed, taking into account the effect of the instant of connecting DC voltage to the field winding on the synchronization process. The calculations were performed

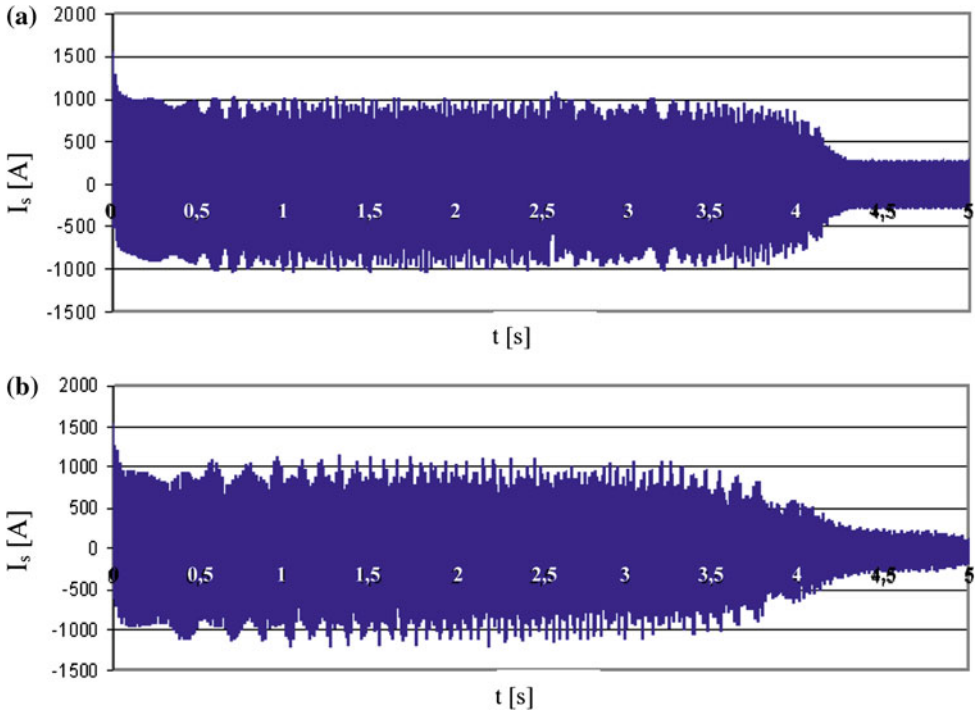

Fig. 3 A diagram of stator phase *A* current during the starting of the unloaded motor ($p = 10$): **a** calculated, **b** measured

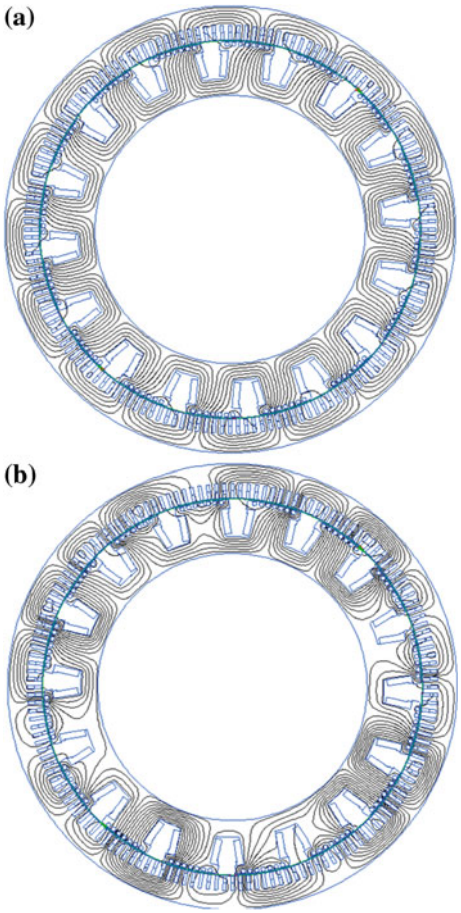

Fig. 4 An image of the electromagnetic field generated by the armature winding of, respectively, the single-speed motor (**a**) and the two-speed motor at $p = 10$ (**b**)

Table 2 The ratings of the WPK 5.3 fan

Rated capacity (m^3/s)	366.6/458.3
Maximum efficiency	0.885
Weight (Mg)	50.438
Inertia (Mg m^2)	37

for load torque changed from 0.45 to $0.8T_N$. This corresponds to the load which the WPK 5.3 fan constitutes with its control unit flaps, closed to fully opened. The rated field voltage and the resultant moment of inertia of the fan drive system: $J_r \approx 40$ Mg m^2 were used in the calculations.

The calculation results show that at a load torque of $0.45--0.5T_N$, the synchronization of the motor is effective regardless of the adopted instant of connecting DC voltage to the field winding. But the instant of synchronization initiation has a significant influence on the dynamic waveforms and synchronization time. It became also apparent that for the load torque of $0.55T_N$, the mutual position of the stator field axis and the rotor field axis at the instant of connecting field voltage determines the effectiveness of synchronization. Figure 5 shows the effect of the synchronization starting instant on the rotational speed waveforms during the synchronization of the motor at this load torque. The broken line marks the particular field voltage connection instants.

An analysis of the calculation results showed that field voltage connection within angle δ of $(-90)^\circ$ to $(-15)^\circ$ (Fig. 5), where δ is the angle between the stator field axis and the rotor field axis, ensures effective synchronization and dynamic waveform attenuation.

For the adopted motor operating conditions ($T_L = 0.55T_N$), the most advantageous synchronization starting instant is an angle δ of about $(-45)^\circ$ (Fig. 5). It ensures effective synchronization during the first cophasality of the armature and field magnet fields. The calculation results also show that the process started at an angle δ of about 90° does not result in effective synchronization and asynchronous operation sets in [6].

Calculations performed for the synchronization of the two-speed motor up to its lower rotational speed at a load torque higher than $0.55T_N$ showed that regardless of the choice of an instant of connecting the rated field voltage, the process runs ineffectively. In such cases, field current forcing is commonly used to increase the pull-in torque. Figure 6 shows the calculated waveforms of armature phase A current I_s, field current I_f, field-winding-terminal voltage U_f, electromagnetic torque and rotational speed during synchronization processes started at angle $\delta = 0^\circ$ and field current forcing. The letter k in the figures represents the scale factors of the individual waveforms of the observed quantities.

According to Fig. 6a, the increase of the field current to $1.5I_{fn}$ at a torque load of $0.6\,T_N$ does not synchronize the motor. For the motor operating conditions, effective synchronization is ensured by a field current above $2.5I_{fn,}$ (Fig. 6b). But the high field current causes considerable electromagnetic torque pulsation resulting in mechanical system overload. Because of the large speed oscillations (Fig. 6b), the transient processes take longer to stabilize whereby synchronization time increases. Besides, to produce such a high forcing current, one must increase the power of the field circuit supply equipment even though its capacity is used for a few seconds during each starting of the motor.

The effectiveness of the synchronization of the motor under considerable torque load can be increased also through field current control in the synchronization initiation–synchronous speed interval. During synchronization, the field current can be controlled by changing the polarization of the field circuit supply DC voltage by means of a transistor switch [9]. In this way, the direction of the current flowing in the field winding can be appropriately changed in a proper instant,

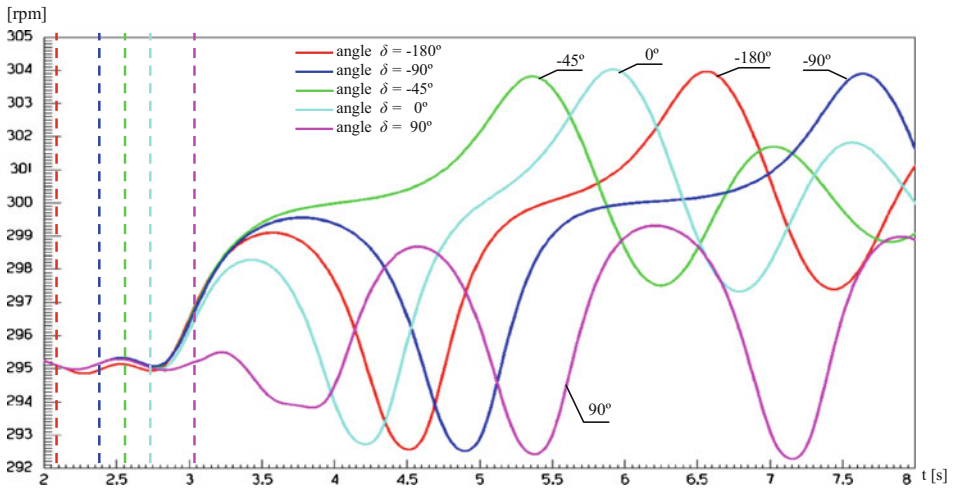

Fig. 5 The effect of the synchronization starting instant on rotational speed waveforms during motor synchronization at a load torque of $0.55T_{\mathrm{N}}$, $p = 10$

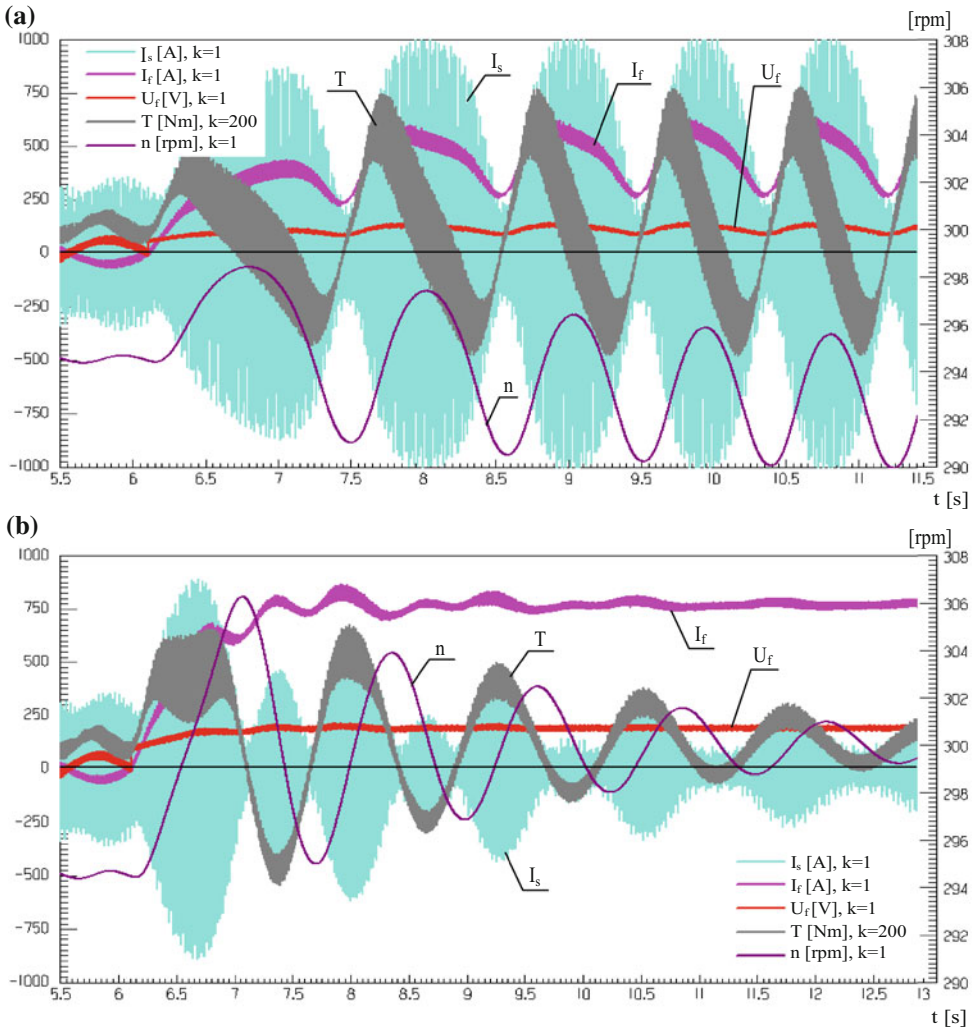

Fig. 6 Waveforms of the quantities during motor synchronization started at: angle $\delta = 0°$, a load torque of $0.6T_{\mathrm{N}}$ and field current forcing of $1.5I_{\mathrm{fn}}$ (**a**) and $2.5I_{\mathrm{fn}}$ (**b**), $p = 10$

influencing the braking torque during the process. Figure 7 shows a diagram of the investigated motor's excitation system incorporating a voltage polarization change system and a protective capacitor.

Figure 8 shows the calculated waveforms of armature phase A current I_{s}, field current I_{f}, field-winding-terminal voltage U_{f}, electromagnetic torque and rotational speed for the synchronization of the investigated motor with the field

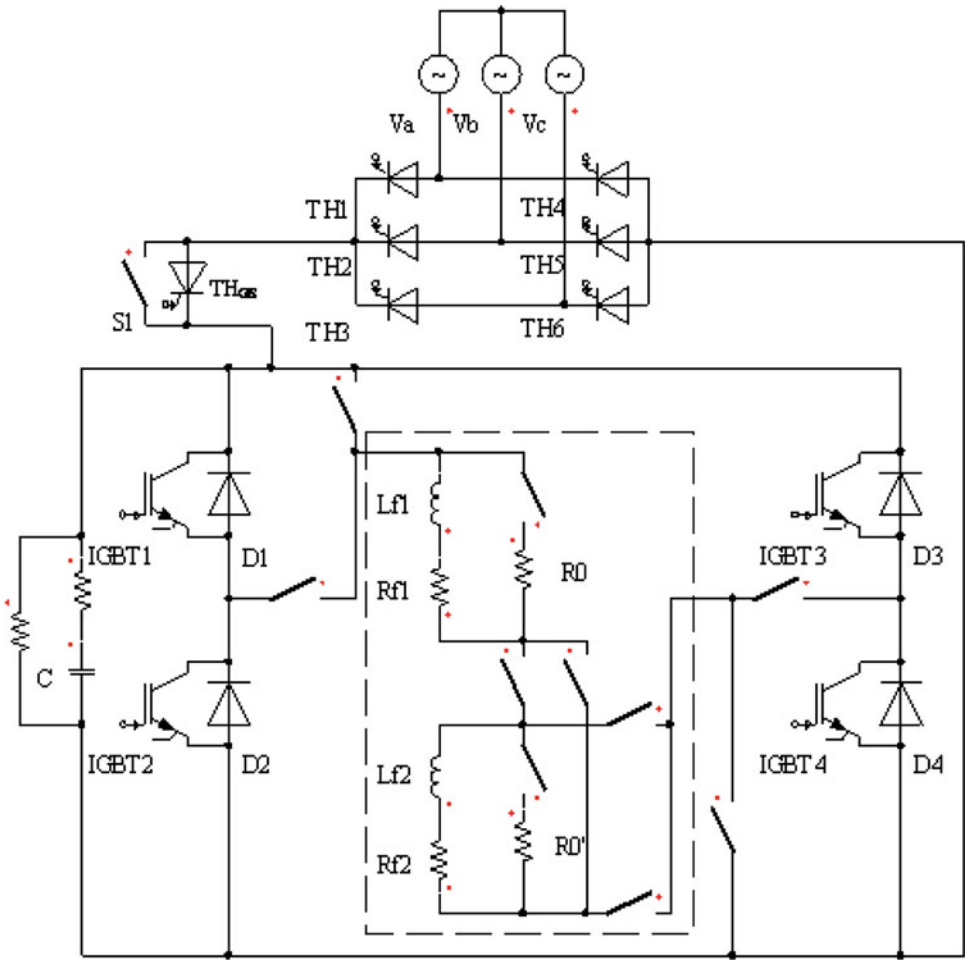

Fig. 7 A diagram of the field winding with an H connected transistor switch and a protective capacitor

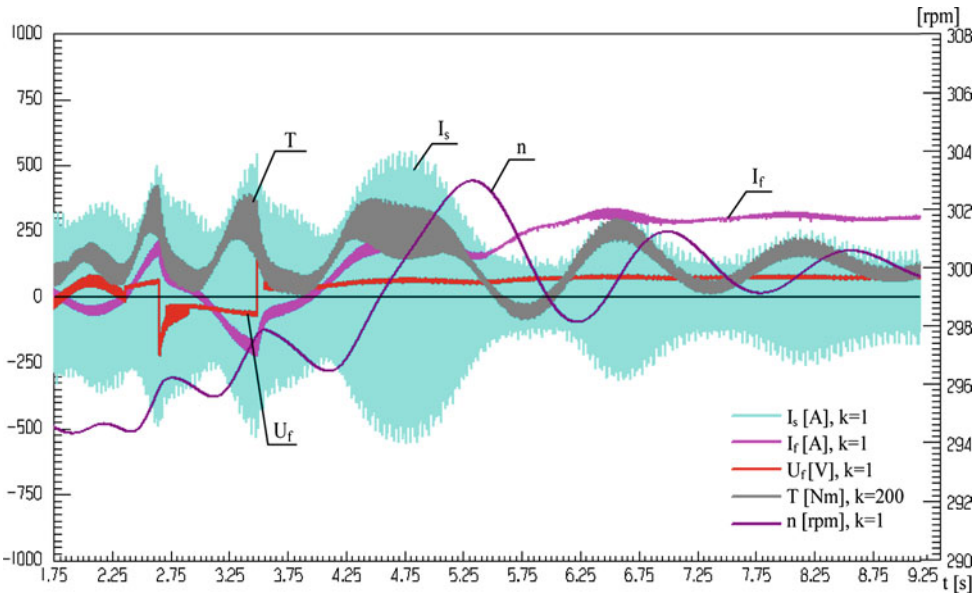

Fig. 8 Waveforms of the quantities during motor synchronization started at angle $\delta = 0°$, a load torque of $0.6T_N$ and field current control from the start until the synchronous speed is reached

voltage change system in the same operating conditions as during synchronization with current $2.5I_{fn}$ (Fig. 6). In the calculations, field voltage polarization was assumed to change at angle $\delta = 90°$ and then at angle $\delta = (-90)°$. Once the synchronous speed is reached, the rated DC voltage (Fig. 8) is switched on.

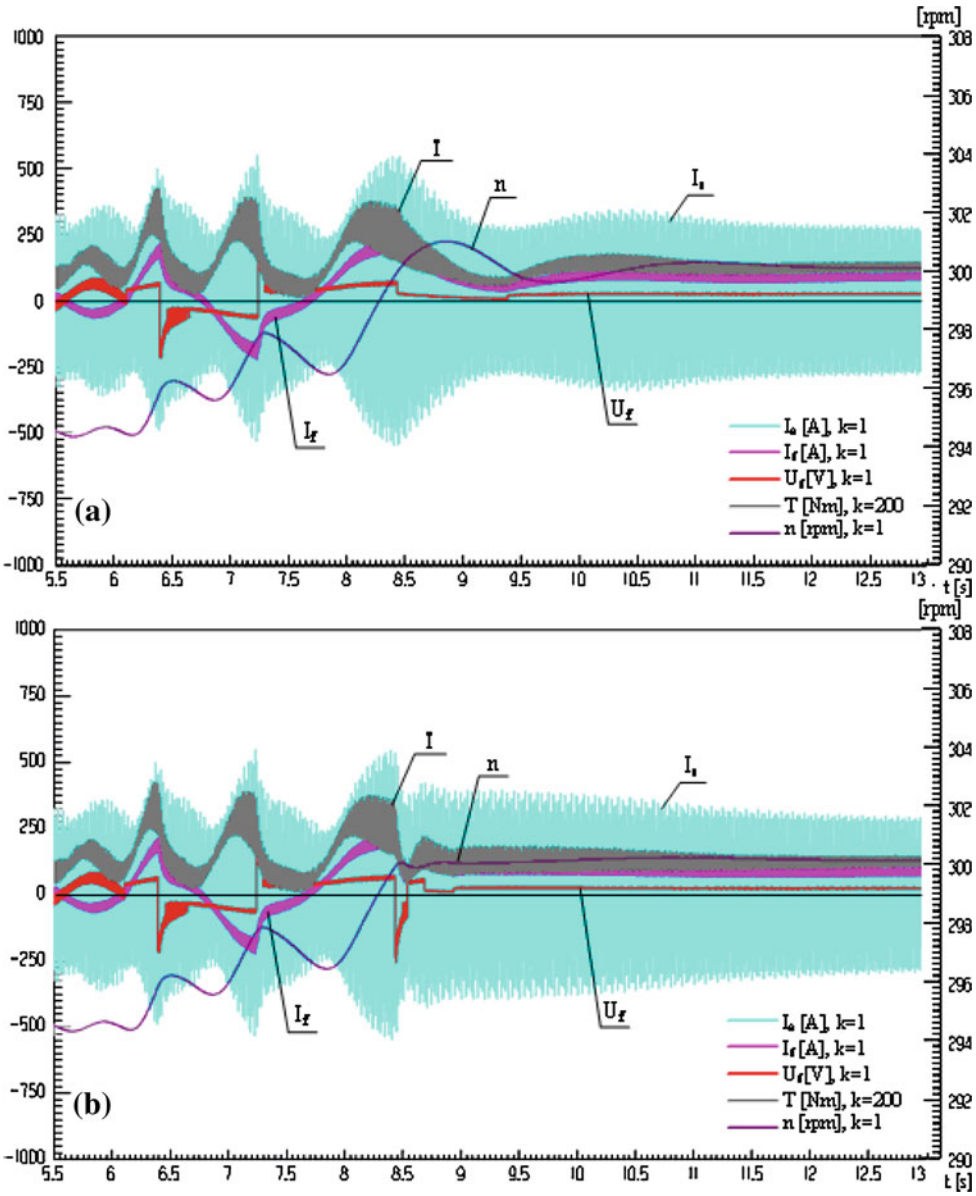

Fig. 9 Waveforms of the quantities during motor synchronization and field current control from the start of synchronization until the synchronous speed is reached, and in the final stage of the process, through jogging (**a**) and supply voltage polarization (**b**)

By controlling the direction of the field current during synchronization, one can produce a dynamic torque for both positive and negative angles δ and so minimize the braking torque and attenuate the dynamic waveforms. The proposed synchronization method (Fig. 8) guarantees effective synchronization and a considerable reduction of armature current, electromagnetic torque and rotational speed fluctuations, which reduces mechanical impacts to the transmission shaft in comparison with the current forcing method. Thanks to current control through field circuit supply voltage polarization, the motor can be synchronized when loaded with a torque 20% higher than the torque at synchronization with current $1.5I_{\mathrm{fn}}$. The adopted control algorithm guarantees effective synchronization at the rated field voltage, whereby the field magnet supply equipment power can be reduced and the process duration is noticeably shorter than in the case of synchronization with current $2.5I_{\mathrm{fn}}$ (Fig. 6b).

Because of the fan drive system's high resultant moment of inertia—ten times higher than that of the drive motor (Tables 1 and 2)—and the constant rated field voltage switched on in the final stage of synchronization, the latter does not end once the motor reaches the synchronous speed (Fig. 8). The elastic interaction between the synchronous torque and the mechanical torque and the moment of inertia [8] causes considerable oscillation of speed around the fixed value (Fig. 8), resulting in considerable electromagnetic torque fluctuations and several times longer synchronization time. This adversely affects the drive system and may result in the premature wear out of the bearings. Rotational speed fluctuation can be reduced and synchroni-

zation time much shortened through the proper control of the field current, also after the motor exceeds the synchronous speed.

Field current can also be controlled through the periodic jogging (inching) of field circuit supply DC voltage or by appropriately changing the polarization of this voltage. Figure 9 shows the calculated waveforms of armature phase A current I_s, field current I_f, field-winding-terminal voltage U_f, electromagnetic torque and rotational speed for the synchronization of the investigated motor in the above operating conditions and for field current control also after the synchronous speed is reached. In the calculations, field current control was performed as a function of instantaneous motor rotational speed. Once the motor reached the synchronous speed, the exciter thyristor control angle was changed to obtain a minimum rectified voltage (Fig. 9a), or the field voltage polarization was changed (Fig. 9b). The field voltage (Fig. 9a) or its polarization (Fig. 9b) was changed again at the instant when the motor speed was lower than the synchronous speed.

Thanks to the methods and algorithm of controlling the field current in the final stage of synchronization, waveform stabilization time can be significantly reduced. Also, electromagnetic torque and rotational speed fluctuations are significantly reduced and limited to positive values (Fig. 9a, b) whereby adverse mechanical impacts to the transmission shaft are minimized.

4 Conclusions

The calculations have shown that through the selection of a proper synchronization initiating instant and through proper field current control, one can increase the effectiveness of the synchronization process, particularly at a high motor load torque. Also electromagnetic torque, armature current and rotational speed fluctuations can be considerably reduced in this way (in comparison with the field current forcing method), ensuring effective motor synchronization at the rated field current. Consequently, the power of the equipment installed in the field magnet supply circuit can be reduced. Field current control in the final stage of synchronization makes it possible to minimize rotational speed pulsation and to reduce motor torque variation amplitude and so to attenuate transients and significantly shorten the synchronization process.

Open Access This article is distributed under the terms of the Creative Commons Attribution Noncommercial License which permits any noncommercial use, distribution, and reproduction in any medium, provided the original author(s) and source are credited.

References

1. Antal L, Zawilak J (2001) A two-speed synchronous motor—technical and economical aspects. In: 37th international symposium on electrical machines SME 2001, Ustroń-Zawodzie, 19–22 June, pp 353–360 (in Polish)
2. Antal L, Zawilak J (2003) Torque of two-speed synchronous motor with switchable armature and field winding. In: 39th international symposium on electrical machines SME 2003. Gdańsk-Jurata, 9–11 June, pp 104–112 (in Polish)
3. Antal L, Zawilak J (1996) Magnetic field of the salient–pole 2–speed synchronous motor. In: Scientific papers of Institute of Electric Machines and Drives of Wrocław University of Technology, no. 44, Studies and Materials, no. 19, Wrocław, pp 11–20 (in Polish)
4. Antal L, Zawilak J (2004) Two speed synchronous motor testing results. In: Exploitation of electrical machines and driver, Ustroń, 19–21 May 2004. Research and Development Centre of Electrical Machines "Komel", no. 68, Katowice, pp 107–112 (in Polish)
5. Kaczmarek T, Zawirski K (2000) Drive systems with synchronous motor, Poznań University of Technology, Poznań (in Polish)
6. Paszek W (1998) Dynamics of electric alternating current machines. Gliwice, Helion (in Polish)
7. Sobczyk T (1984) Gentle synchronization of high-power synchronous motors out of asynchronous operation. In: 20th international symposium on electrical machines SME 1984, synchronous machine, Kazimierz Dolny, pp 28–29 (in Polish)
8. Zalas P, Zawilak J (2006) Soften and reduction duration of synchronization process in synchronous motors. 42th international symposium on electrical machines SME 2006, Krakow, 3–6 July, pp 355–358 (in Polish)
9. Zalas P, Zawilak J (2006) Influence of system control of excitation current value on synchronization process in synchronous motors. In: Exploitation of electrical machines and driver, Ustroń, 17–19 May 2006, Research and Development Centre of Electrical Machines "Komel", no. 75, Katowice, pp 83–88, [in Polish]
10. Zalas P, Zawilak J (2005) Selection of excitation start-up moment during synchronization process in synchronous motors. In: Exploitation of electrical machines and driver, Ustroń, 18–20 May 2005, Research and Development Centre of Electrical Machines "Komel", no. 71, Katowice, pp 59–64 (in Polish)
11. Zalas P (2007) Analysis of synchronization process of synchronous motors with asynchronous starting. PhD dissertation, Wrocław University of Technology, Wrocław (in Polish)
12. Zawilak J (1986) Pole-changing windings of A.C. machine. In: Scientific papers of Institute of Electromachine Systems of Wrocław University of Technology, no. 37, series M, no. 7, Wrocław (in Polish)
13. Zhou P, Stanton S, Cendes ZJ (1999) Dynamic modeling of three phase and single phase induction motors. In: Electric machines and drives, 1999. International Conference IEMD '99, 9–12 May, pp 556–558